Bond behavior between glulam and GFRP's using direct pullout tests

Marco Jorge
MSc, Technician, Dep. of Civil Engrg.
Univ. of Minho (Guimarães)
marco@civil.uminho.pt

José Sena-Cruz
PhD, Assistant Professor, Dep. of Civil Engrg.
Univ. of Minho (Guimarães)
jsena@civil.uminho.pt

Jorge Branco
PhD, Assistant Professor, Dep. of Civil Engrg.
Univ. of Minho (Guimarães)
jbranco@civil.uminho.pt

Joaquim Barros
PhD, Associate Professor, Dep. of Civil Engrg.
Univ. of Minho (Guimarães)
barros@civil.uminho.pt

Gláucia Dalfré
PhD student, Dep. of Civil Engrg.
Univ. of Minho (Guimarães)
gmdalfre@civil.uminho.pt

Palavras-chave – Glulam; varões de polímeros reforçados com fibras de vidro; técnica NSM; ensaios de arrancamento directo
Keywords – Glulam; GFRP rods; NSM strengthening technique; direct pullout tests

RESUMO

Com o objectivo de avaliar o comportamento da ligação entre lamelados colados e varões de GFRP, quando aplicados de acordo com a técnica NSM, foi realizado um programa de ensaios experimentais com recurso a ensaios de arrancamento directo. Neste programa experimental foram analisadas três variáveis: o tipo de GFRP (2 tipos), a localização do FRP/dimensão da ranhura (2 tipos) e o comprimento de amarração (L_b=30 mm, 60 mm, 120 mm e 180 mm). A instrumentação inclui a medição dos deslizamentos na zona solicitada e na extremidade livre, bem como da força de arranque. Trinta e sete provetes foram ensaiados sob controlo de deslocamento com recurso a um sistema servo-controlado. O presente trabalho descreve os ensaios e apresenta e discute os resultados obtidos.

ABSTRACT

To evaluate the bond behavior between glulam and GFRP rods using the near-surface mounted (NSM) strengthening technique, an experimental program was carried out by means of direct pullout tests. In this experimental program three variables were analyzed: the GFRP type (2 types),

the GFRP location/groove size (2 types) and the bond length (L_b=30 mm, 60 mm, 120 mm and 180 mm). The instrumentation includes the loaded and free end slips, as well as the pullout force. Thirty seven specimens were tested under displacement control using a servo controlled equipment. In this work the tests are described, and the obtained results are presented and discussed.

1. Introduction

Considering the impressive amount of resources necessary to rehabilitate deteriorated infrastructures (bridges, buildings, etc.), it is important to find effective and economic strategies to maintain in use these structures. Strengthening techniques based on FRP materials have been proposed since 1990's, having been initially applied to concrete structures, but their use was rapidly extended to masonry, timber and steel structures.

The externally bonded reinforcement (EBR), the near-surface mounted (NSM) technique (ACI 2008), and the mechanically fastened FRP (MF-FRP) (Bank 2004) are the most known strengthening techniques using FRP systems. In the context of any strengthening technique, bond behavior is an important issue, since it governs the fundamental design equations. The bond performance influences not only the ultimate load-carrying capacity of a reinforced element but also some serviceability aspects, such as deformation. In the last decades several test methods have been proposed and used in the bond research, mainly in concrete material. The most common are the direct and the beam pullout tests. At the present time, there is no general agreement about the correct test setup to assess the bond behavior for the distinct FRP systems (Barros and Costa 2010).

To study the bond behavior between glulam and GFRP (glass fiber reinforced polymers) rods applied according to the near-surface mounted (NSM) strengthening technique, an experimental program composed of direct pullout tests was carried out. The influence of GFRP type, the groove geometry/FRP location and the bond length, on the bond behavior was investigated. In the following sections the performed tests are described in detail, and the obtained results are presented and discussed.

2. Experimental Program

2.1. Specimens and Test Configuration

The experimental program was composed of thirty seven direct pullout bond tests, grouped in series of three or six specimens. Bond lengths ranging between 30 and 180 mm were adopted in order to assess its influence on the bond behavior. The lower bond length value, 30 mm, was considered since the bond length must be large enough to be representative of the glulam-FRP's interface conditions and to make negligible the unavoidable end effects. The upper bound was limited to 180 mm due to limitations associated to the specimen's geometry.

The code names given to the test series consist on alphanumeric characters separated by underscores (see Table 1). The first string indicates the GFRP type (GFRP1 and GFRP2). The second string defines the depth at which the FRP was installed into the groove (D1 and D2). Finally, the last string indicates the bond length in millimeters (for instance, Lb30 represents a specimen with a bond length of 30 mm).

Fig. 1 shows the specimen geometry and the direct pullout test configuration of all the series tested. The specimen consists of a glulam block of $140 \times 200 \times 400$ mm^3 dimensions, in which a FRP is embedded.

The bond test region was located in the upper part of the block, and several bond lengths, L_b, were analyzed (see Table 1). To avoid a premature splitting failure in the glulam ahead the loaded end, the bond length started 50 mm far from the block end.

The instrumentation of the specimens consisted on three linear variable differential transducers (LVDT) and a load cell. The LVDT1 was used to control the test, at 2 μm/s slip rate, and to measure the slip at the loaded end, s_l, while the displacement transducer LVDT2 was used to measure the slip at the free end, s_f. The LVDT3 was used to measure the rotation of the specimen.

The applied force, *F*, was registered by a load cell placed between the specimen top surface and the actuator.

Material	Depth (mm)	L_b (mm)	Denomination	Number of specimens
GFRP1	15	30	GFRP1_D1_Lb30	6
		60	GFRP1_D1_Lb60	6
		120	GFRP1_D1_Lb120	6
	20	30	GFRP1_D2_Lb30	2
		60	GFRP1_D2_Lb60	2
		120	GFRP1_D2_Lb120	3
		180	GFRP1_D2_Lb180	2
GFRP2	15	30	GFRP2_D1_Lb30	3
		60	GFRP2_D1_Lb60	3
		120	GFRP2_D1_Lb120	4

Table 1 – Experimental program

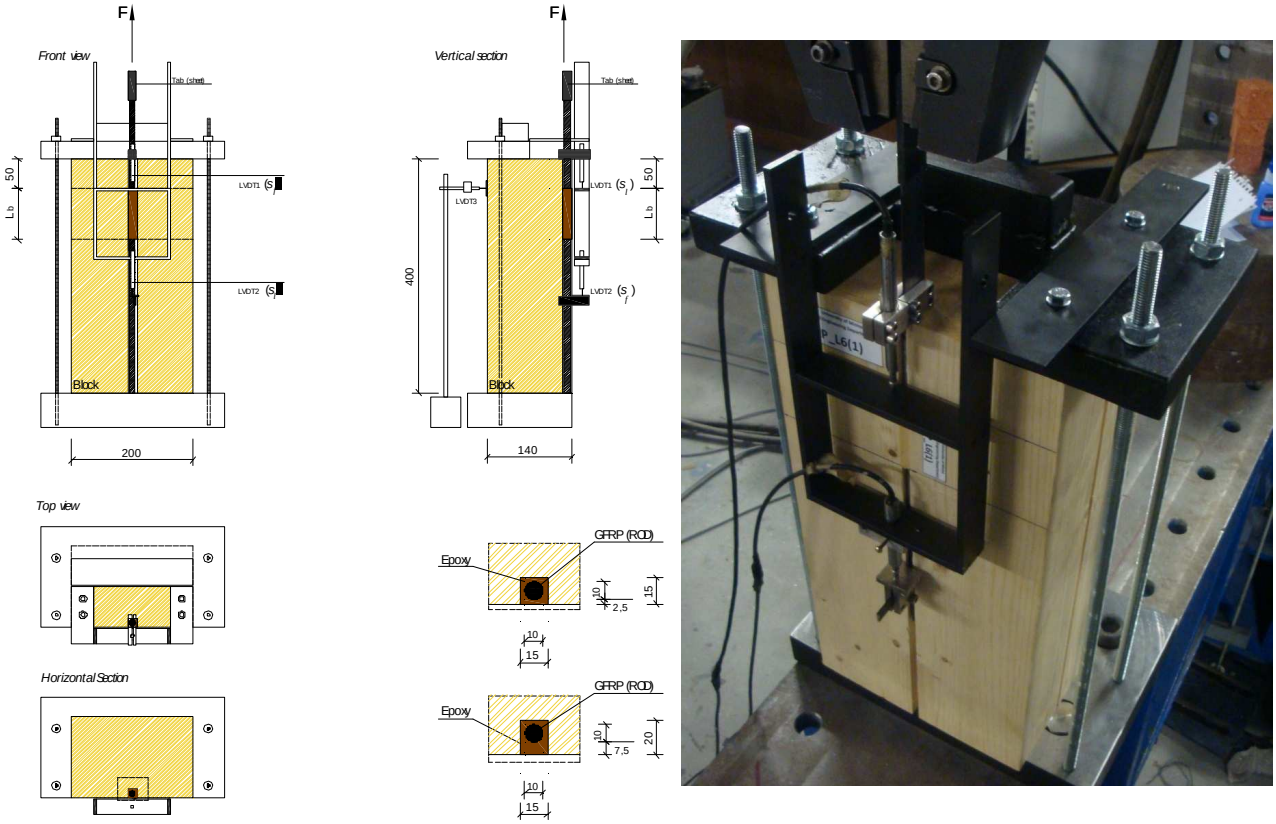

Figure 1 – Specimen geometry and direct pullout test configuration. Note: all dimensions are in [mm].

2.2. Material characterization

2.2.1. Timber

In the present experimental program glued laminated timber, currently named by glulam, of strength class GL24h (NP EN 1194:1999), was used for all the series. The material characterization of the GL24h included compression and tensile tests parallel to the grain, according to EN 408 (CEN 2003). From the compression tests, an average compressive strength of 27.99 MPa with a coefficient of variation (CoV) of 17.6%, and an average modulus of elasticity of 6.62 GPa (CoV=27.8%) were obtained.

From the tension tests, an average tensile strength, modulus of elasticity and strain at the peak stress of 55.93 MPa (CoV=16.7%), 9.17 GPa (CoV=11.9%) and 6.35‰ (CoV=12.4%) were obtained.

2.2.2. GFRP rod

The GFRP rod used in the present work, with a trademark Maperod G, was provided in rolls of 6 meters each, and was supplied by MAPEI®. Two distinct types of Maperod G were used with different external surface (see Fig. 2). Herein, the rod with a rougher external surface was denominated as GFRP2, whereas the other as GFRP1. These rods have a diameter of 10 mm and the external surface is sand blasted.

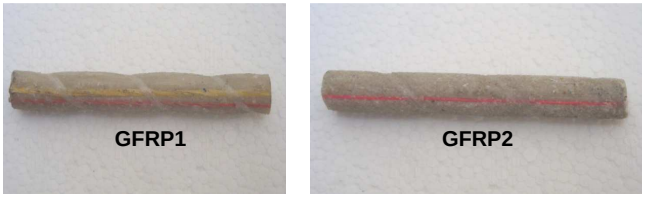

Figure 2 – GFRP used in the experimental program

Tensile tests were carried out to assess the tensile mechanical properties of each GFRP rod type, according to ISO TC 71/SC 6 N - Part 1 - (2003). Tests were performed under a displacement rate of 2 mm/min. To measure the modulus of elasticity, a clip gauge was mounted at middle region of each specimen. The results obtained from the mechanical characterization of the GFRP rods are presented in Table 2. Both GFRP rods have similar response, not only in terms of tensile strength but also in terms of modulus of elasticity. Nevertheless GFRP2 presents a modulus of elasticity slightly higher. Very low values of the coefficients of variation (CoV) were obtained for the case of GFRP1, but a rather high value of CoV was registered for the strain at the maximum tensile stress for the GFRP2.

GFRP	F_{fmax} (kN)	σ_{fmax} (MPa)	E_f (GPa)	ε_{fmax} (‰)	***Failure mode***
GFRP1	61.12 (3.5%)	778.14 (3.5%)	38.42 (1.3%)	20.25 (2.3%)	XGM (all)
GFRP2	61.15 (1.6%)	786.04 (2.8%)	41.60 (7.8%)	18.99 (10.2%)	OGM (all)

Notes: F_{fmax}= maximum force; $\sigma=F/(\pi\times10^2/4\ mm^2)$; σ_{fmax}= tensile strength; E_f = longitudinal elasticity modulus; ε_{fmax}= strain at σ_{fmax}; $\varepsilon_{fmax}=\sigma_{fmax}/E_f$; E_f is the slope of curve σ–ε between 20% and 50% of σ. Failure modes: XGM – Explosive failure in gauge measuring length; OGM – Failure located outside of the gauge measuring length. The values between parentheses are the corresponding coefficients of variation.

Table 2 – Main results obtained on the mechanical characterization of the GFRP rods (average values)

2.2.3. Epoxy adhesive

In the present experimental work the epoxy MapeWood Paste 140, supplied by MAPEI®, was used. This thixotropic epoxy adhesive is currently used for the restoration of timber structural elements, and is composed of two premeasured parts (Part A = resin and Part B = hardener).

To assess the mechanical properties of each hardened adhesives, tensile tests were carried out according to ISO 527-2 (1993). After casted, the specimens were kept in the laboratory environment, and when tested they had the same age of the adhesive of the pullout tests. The adhesive specimens were tested in a universal test machine, at a displacement rate of 1 mm/min. A clip gauge mounted on the middle zone of the specimen recorded the strains, whereas a high accuracy cell load has registered the applied force. Table 3 includes the main obtained results.

Adhesive	$F_{adh,max}$ (kN)	$\sigma_{adh,max}$ (MPa)	E_{adh} (GPa)	$\varepsilon_{adh,max}$ (‰)	***Failure mode***
MapeWood Paste 140	0.69 (8.4%)	17.15 (7.5%)	8.11 (17.6%)	2.60 (19.6%)	OR (3) + IR (3)

Notes: $F_{adh,max}$= maximum force; $\sigma_{adh,max}$= uniaxial tensile strength; E_{adh}= longitudinal elasticity modulus; $\varepsilon_{adh,max}$= strain at σ_{fmax}; E_{adh} is the slope of the curve σ–ε between 0.0025 and 0.0075 of ε. Failure modes: IR - inside the clip gauge region; OR - outside the clip gauge region; GR grip region. The values between parentheses are the corresponding coefficients of variation.

Table 3 – Main results obtained on the mechanical characterization of the adhesive (average values)

2.3. Preparation of Specimens

The glulam blocks used for the NSM bond tests were supplied with the correct dimensions including the groove's geometry. For the series D1 the grooves had a width and a depth of about 15 mm and 15 mm, respectively, while for the case of D2 series these values were 15 mm and 20 mm.

Some details of glulam and FRP's preparations just before the strengthening are shown in Fig. 3. These procedures include the following main steps:

i. A sandpaper was used to eliminate the wood chips inside the grooves formed during the sawing process;
ii. The grooves were cleaned using compressed air;
iii. A masking procedure in the vicinity of the bonding areas was adopted to keep original aesthetic of the glulam surface after strengthening;
iv. A small tab, built with FRP material, was fixed at the loaded end to measure the loaded end slip;
v. Small latex delimiter pieces were made to assure the correct location of the FRP in the groove cross-section;
vi. To guarantee the desired bond lengths, pieces of plastic were glued on FRP's surfaces;
vii. On the bond region of the glulam blocks and the FRP's were cleaned with acetone to remove any possible dirt.

The rods were fixed to the glulam grooves using the MapeWood Paste 140 epoxy adhesive. Fig. 3 also shows the main steps required to strengthen the glulam specimens. Preparation of the epoxy adhesive was performed according to the recommendations of the supplier. The grooves were filled with the epoxy adhesive using a spatula, and GFRP rods are cover with a thin layer of epoxy adhesive. Then, the FRP's were gradually inserted into the grooves and slightly pressed to force the epoxy adhesive to flow between the FRP and the groove sides. Finally, the epoxy adhesive in excess was removed and the surface was leveled.

The specimens were kept in the laboratory environment before being tested. The pullout tests were carried out at least 10 days after the application of the FRP reinforcement.

3. Results and Discussion

The analysis is focused in the following results: maximum force, free and loaded end slips at the peak load, average bond stress, and failure modes. In addition, the relationship between the pullout force and the loaded end slip is also analyzed. As already mentioned, the two types of GFRP rods used had similar mechanical properties, but GFRP2 had rougher external surface.

Figs. 4 to 6 show the average pullout force versus loaded end slip ($F_l - s_l$) relationships for the series GFRP1_D1, GFRP2_D1 and GFRP1_D2, respectively. In the test groups with GFRP1 rods a softening response occurred for the series with L_b=30 and 60 mm, while in the GFRP2 test group only a small softening branch has occurred in the series with L_b=30 mm. For the L_b=120 mm and 180 mm the pullout load has increased with the loaded end slip up to failure, regardless the type of GFRP. Comparing the performance of GFRP1 and GFRP2 (see Figs. 4 and 5) a higher performance was attained for the case of GFRP2, e.g. for L_b= 120 mm the maximum load is approximately equal to 25 kN and 30 kN for the case of GFRP1 and GFRP2, respectively. The superior behavior of GFRP2 can be attributed to the type of external surface of this rod. Comparing the D1 and D2 series, a more linear $F_l - s_l$ relationship was obtained in the former, but the most relevant point is the increase in the pullout capacity that was obtained when the GFRP rod is deeper installed into the groove, which is in agreement with results obtained with NSM CFRP laminates (Costa and Barros 2011).

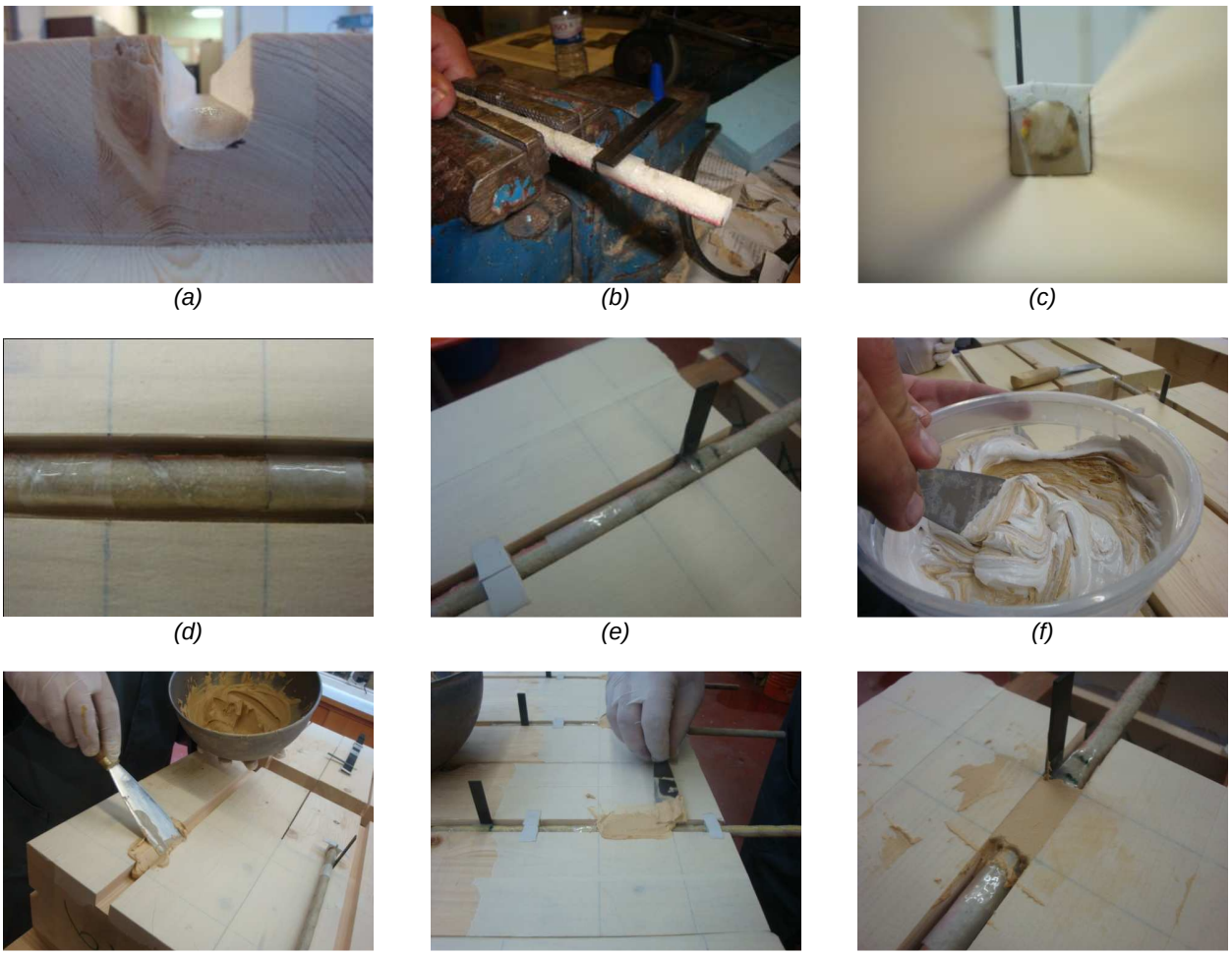

(a) *(b)* *(c)*

(d) *(e)* *(f)*

(g) *(h)* *(i)*

Figure 3 – (a) Detail of the groove after liming; (b) FRP tab to measure the loaded end slip; (c) latex delimiters; (d) final state of the bond zone; (e) final state of the materials before the application of the strengthening; (f) epoxy adhesive preparation; (g) application of epoxy adhesive in the groove; (h) leveling the surface; (h) final state of the specimens before removing the mask

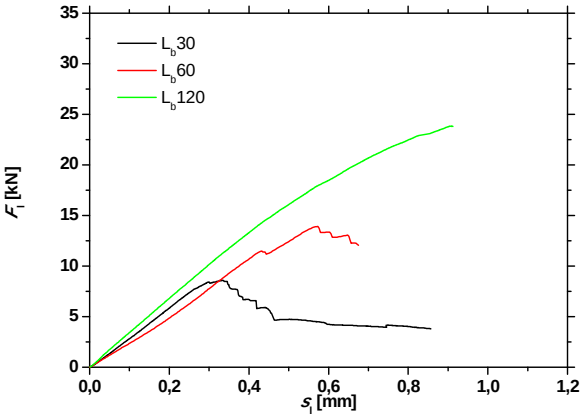

Figure 4 – Pullout force vs. loaded end slip for the series GFRP1_D1 (average curves)

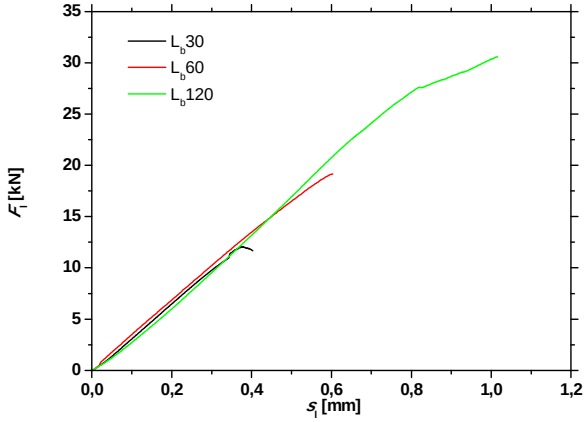

Figure 5 – Pullout force vs. loaded end slip for the series GFRP2_D1 (average curves)

Tables 4, 5 and 6 present the main results obtained for the series GFRP1_D1, GFRP1_D2 and GFRP2_D1, respectively. As expected, the maximum pullout force, F_{fmax}, and the corresponding loaded end slip, s_{fmax}, have increased with the bond length. The pullout efficiency, defined by the F_{fmax} / F_{fu} ratio, was approximately equal to 65% for the GFRP1_D2_Lb180-2 (second specimen of the GFRP1_D2 series with a bond length of 180 mm). In general, all the parameters present quite low values of the corresponding coefficients of variation. The exception is for the values of slips at the loaded and free ends. In fact high coefficients of variation were observed, and main reason for that can be attributed to the difficulty in measuring this physical entity.

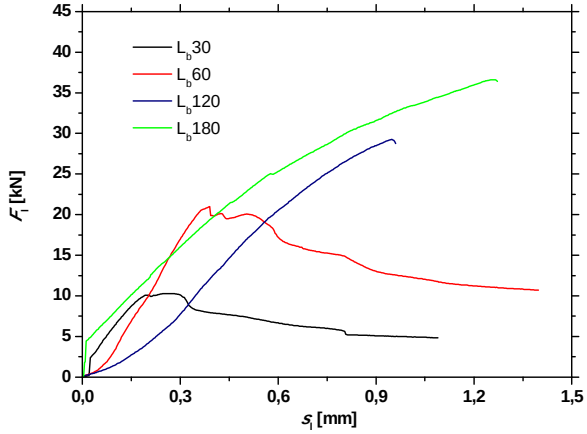

Figure 6 – Pullout force vs. loaded end slip for the series GFRP1_D2 (average curves)

Specimen	F_{fmax} (kN)	F_{fmax} / F_{fu} (%)	$\tau_{max,av1}$ (MPa)	$\tau_{max,av2}$ (MPa)	s_{fmax} (mm)	s_{lmax} (mm)	***Failure mode***
GFRP1_D1_Lb30-1	8.78	14.37	9.32	6.40	0.205	0.328	FAI+SPL
GFRP1_D1_Lb30-4	9.19	15.04	9.75	6.76	0.277	0.366	FAI+SPL
GFRP1_D1_Lb30-5	9.46	15.48	10.04	6.86	0.224	0.264	FAI+SPL
GFRP1_D1_Lb30-6	10.06	16.47	10.68	7.34	0.259	0.345	FAI+SPL
GFRP1_D1_Lb30-7	9.85	16.12	10.45	7.21	0.296	0.441	FAI+SPL
GFRP1_D1_Lb30-8	10.14	16.59	10.76	7.28	0.256	0.321	FAI+SPL
GFRP1_D1_Lb30	**9.58 (5.6%)**	**15.68 (5.6%)**	**10.17 (5.6%)**	**6.97 (5.3%)**	**0.25 (13.2%)**	**0.34 (17.0%)**	-
GFRP1_D1_Lb60-1	14.03	22.95	7.44	5.08	0.250	0.420	FAI+SPL
GFRP1_D1_Lb60-2	16.05	26.27	8.52	5.83	0.275	0.560	FAI+SPL
GFRP1_D1_Lb60-4	16.16	26.44	8.57	5.91	0.221	0.598	FAI+SPL
GFRP1_D1_Lb60-7	17.67	28.91	9.37	6.40	0.332	0.685	FAI+SPL
GFRP1_D1_Lb60-8	17.74	29.03	9.41	6.49	0.350	0.660	FAI+SPL
GFRP1_D1_Lb60-9	19.71	32.24	10.45	7.11	0.403	0.770	FAI+SPL
GFRP1_D1_Lb60	**16.89 (11.4%)**	**27.64 (11.4%)**	**8.96 (11.4%)**	**6.13 (11.3%)**	**0.31 (22.3%)**	**0.62 (19.5%)**	-
GFRP1_D1_Lb120-1	24.29	39.74	6.44	4.36	0.289	0.954	FAI+SPL
GFRP1_D1_Lb120-2	22.57	36.93	5.99	4.14	0.265	0.832	FAI+SPL
GFRP1_D1_Lb120-3	25.65	41.97	6.80	4.67	0.287	0.891	FAI+SPL
GFRP1_D1_Lb120-4	24.59	40.23	6.52	4.51	0.308	0.867	FAI+G+SPL
GFRP1_D1_Lb120-6	22.91	37.48	6.08	4.10	0.292	0.975	FAI+SPL
GFRP1_D1_Lb120-7	25.00	40.90	6.63	4.55	0.309	0.665	FAI+SPL
GFRP1_D1_Lb120	**24.17 (5.0%)**	**39.54 (5.0%)**	**6.41 (5.0%)**	**4.39 (5.3%)**	**0.29 (5.5%)**	**0.86 (12.9%)**	-

Notes: F_{fmax}= maximum pullout force; F_{fu}= FRP strength force; $\tau_{max,av1}$= average bond stress at the bar-epoxy interface at F_{fmax}; $\tau_{max,av2}$= average bond stress at the glulam-epoxy interface at F_{fmax}; s_{fmax}= free end slip at F_{fmax}; s_{lmax}= loaded end slip at F_{fmax}; FAI – FRP/adhesive interfacial sliding; GAI – glulam/adhesive interfacial sliding; SPL – adhesive splitting; GS – glulam shear failure; CR – adhesive cracking; FF – FRP failure.

Table 4 – Main results obtained in the series GFRP1_D1

Specimen	F_{fmax} (kN)	F_{fmax} / F_{fu} (%)	$\tau_{max,av1}$ (MPa)	$\tau_{max,av2}$ (MPa)	s_{fmax} (mm)	s_{lmax} (mm)	*Failure mode*
GFRP1_D2_Lb30-2	11.45	18.55	12.15	6.86	0.124	0.180	GAI+FAI
GFRP1_D2_Lb30-3	10.75	17.41	11.41	6.43	0.119	0.250	GAI
GFRP1_D2_Lb30	**11.10 (4.5%)**	**17.98 (4.5%)**	**11.78 (4.5%)**	**6.65 (4.6%)**	**0.12 (2.7%)**	**0.21 (23.1%)**	-
GFRP1_D2_Lb60-1	22.68	36.74	12.03	6.75	0.179	0.368	FAI+CR
GFRP1_D2_Lb60-3	22.98	37.23	12.19	6.84	0.253	0.509	G
GFRP1_D2_Lb60	**22.83 (0.9%)**	**36.98 (0.9%)**	**12.11 (0.9%)**	**6.79 (0.9%)**	**0.22 (24.2%)**	**0.44 (22.8%)**	-
GFRP1_D2_Lb120-1	29.79	48.26	7.90	4.43	0.155	0.881	GAI
GFRP1_D2_Lb120-2	31.86	51.61	8.45	4.75	0.216	1.130	GAI+FAI
GFRP1_D2_Lb120-3	32.23	52.21	8.55	4.83	0.235	1.037	GAI+GS
GFRP1_D2_Lb120	**31.29 (4.2%)**	**50.69 (4.2%)**	**8.30 (4.2%)**	**4.67 (4.6%)**	**0.20 (20.6%)**	**1.02 (12.4%)**	-
GFRP1_D2_Lb180-2	40.15	65.04	7.10	4.00	0.110	1.356	GS
GFRP1_D2_Lb180-3	35.41	57.36	6.26	3.51	0.190	1.251	FAI
GFRP1_D2_Lb180	**37.78 (8.9%)**	**61.20 (8.9%)**	**6.68 (8.9%)**	**3.76 (9.1%)**	**0.15 (37.8%)**	**1.30 (5.7%)**	-

Notes: F_{fmax}= maximum pullout force; F_{fu}= FRP strength force; $\tau_{max,av1}$= average bond stress at the bar-epoxy interface at F_{fmax}; $\tau_{max,av2}$= average bond stress at the glulam-epoxy interface at F_{fmax}; s_{fmax}= free end slip at F_{fmax}; s_{lmax}= loaded end slip at F_{fmax}; FAI – interfacial failure FRP/adhesive; GAI – interfacial failure glulam/adhesive; SPL – adhesive splitting; GS – glulam shear failure; CR – adhesive cracking; FF – FRP failure.

Table 5 – Main results obtained in the series GFRP1_D2

Specimen	F_{fmax} (kN)	F_{fmax} / F_{fu} (%)	$\tau_{max,av1}$ (MPa)	$\tau_{max,av2}$ (MPa)	s_{fmax} (mm)	s_{lmax} (mm)	*Failure mode*
GFRP2_D1_Lb30-2	12.08	19.57	12.82	8.74	0.275	0.379	FAI+GAI+SPL
GFRP2_D1_Lb30-3	10.70	17.34	11.36	7.88	0.330	0.346	GAI
GFRP2_D1_Lb30-9	12.75	20.65	13.52	9.33	0.372	0.239	FAI+SPL
GFRP2_D1_Lb30	**11.84 (8.8%)**	**19.18 (8.8%)**	**12.57 (8.8%)**	**8.65 (8.4%)**	**0.33 (15.0%)**	**0.32 (22.9%)**	-
GFRP2_D1_Lb60-3	20.66	33.47	10.96	7.44	0.302	0.667	FAI+GAI+SPL
GFRP2_D1_Lb60-5	19.69	31.89	10.44	7.11	0.367	0.599	GAI+FAI
GFRP2_D1_Lb60-6	20.16	32.66	10.70	7.34	0.410	0.715	GAI+GS
GFRP2_D1_Lb60	**20.17 (2.4%)**	**32.67 (2.4%)**	**10.70 (2.4%)**	**7.30 (2.3%)**	**0.36 (15.1%)**	**0.66 (8.8%)**	-
GFRP2_D1_Lb120-5	32.05	51.91	8.72	6.03	0.309	0.903	FAI+CR
GFRP2_D1_Lb120-8	30.08	48.73	8.5	5.82	0.344	1.024	FAI+SPL
GFRP2_D1_Lb120-9	30.77	49.84	8.16	5.63	0.375	1.050	FAI+SPL
GFRP2_D1_Lb120-10	32.86	53.23	7.98	5.51	0.359	1.050	FAI+SPL
GFRP2_D1_Lb120	**31.44 (4.0%)**	**50.93 (4.0%)**	**8.34 (4.0%)**	**5.75 (4.0%)**	**0.35 (8.1%)**	**1.01 (7.0%)**	-

Notes: F_{fmax}= maximum pullout force; F_{fu}= FRP strength force; $\tau_{max,av1}$= average bond stress at the bar-epoxy interface at F_{fmax}; $\tau_{max,av2}$= average bond stress at the glulam-epoxy interface at F_{fmax}; s_{fmax}= free end slip at F_{fmax}; s_{lmax}= loaded end slip at F_{fmax}; FAI – interfacial failure FRP/adhesive; GAI – interfacial failure glulam/adhesive; SPL – adhesive splitting; GS – glulam shear failure; CR – adhesive cracking; FF – FRP failure.

Table 6 – Main results obtained in the series GFRP2_D1

Fig. 7 shows the principal failure modes obtaine: (i) glulam shear failure (GS); (ii) glulam/adhesive interfacial sliding (GAI); (iii) FRP/adhesive interfacial sliding and adhesive splitting (FAI+SPL).

GS – Glulam shear failure

GAI – Glulam/adhesive interfacial sliding

FAI+SPL – FRP/adhesive interfacial sliding + adhesive splitting

Figure 7 – Typical failure modes obtained

Fig. 8 presents the influence of the bond length (L_b) on the following parameters: pullout force efficiency (F_{max} / F_{fu}), loaded end slip (s_l), average bond strength at FRP/adhesive interface (τ_{av1}), and average bond strength at adhesive/glulam interface (τ_{av2}). From this graphs it can be concluded the following:

- The F_{max} / F_{fu} ratio and the s_l increase with the bond length. Larger L_b values need to be investigated to obtain the maximum values of these parameters;
- Deeper installation of the GFRP rods provided larger F_{max} / F_{fu} and τ_{av1}, regardless the L_b;
- For bond lengths L_b=30 and 60 mm, D2 series presents higher stiffness, when compared with D1 series (see Fig. 8(b)). However, for the case of L_b=120 mm, significant increase in terms of deformation can be observed;
- As expected, average bond strengths Fig. 8(c) and (d) decrease with the increase of L_b.

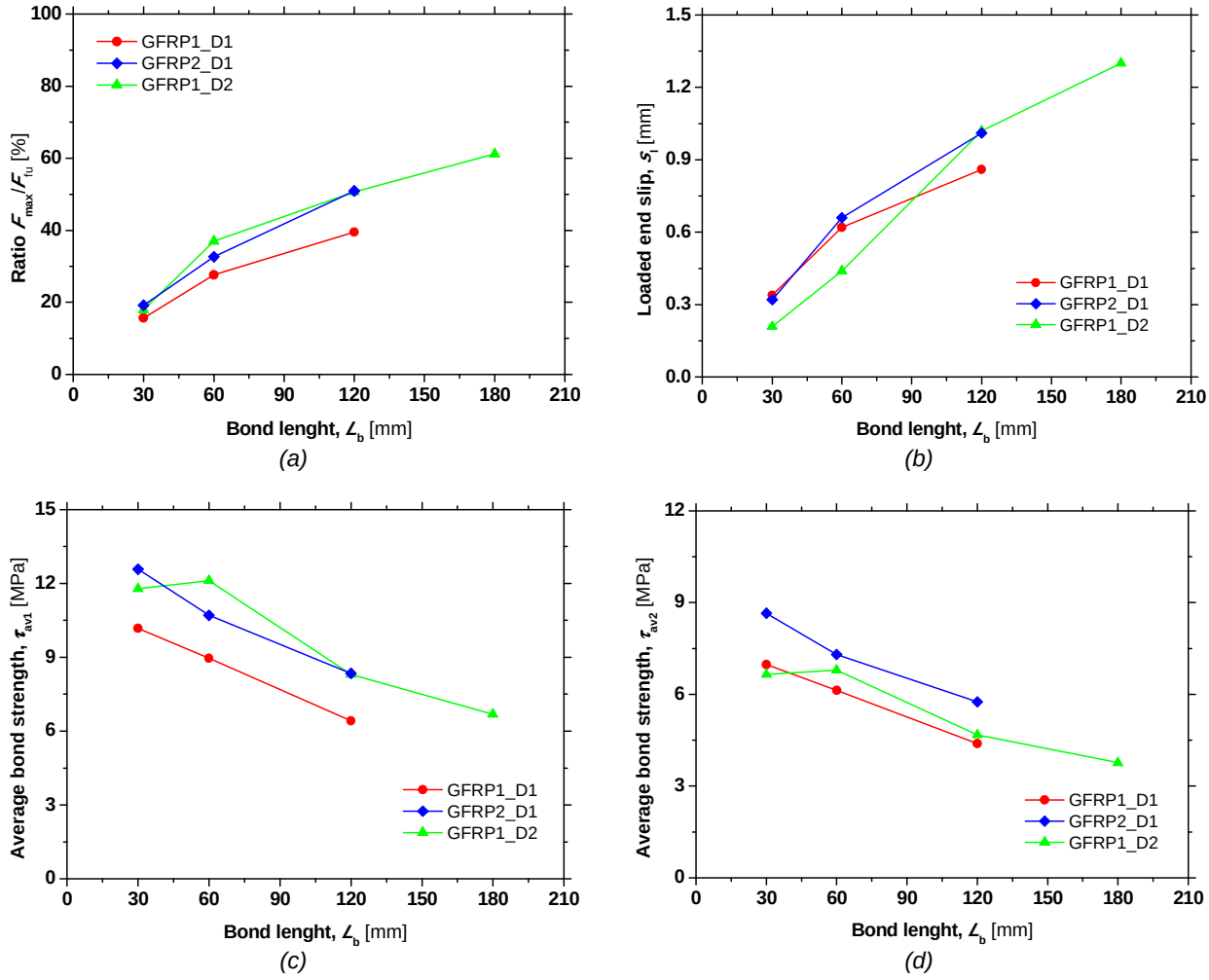

Figure 8 – Bond length influence on: (a) efficiency in terms of maximum load; (b) loaded end slip; (c) average bond strength τ_{av1}; (d) average bond strength τ_{av2}

Conclusions

An experimental study on the bond behavior between GFRP rods and glulam through direct pullout tests, using the near surface mounted strengthening technique, was presented. The main parameters studied were: the surface type of GFRP rod, the depth of the rod into the groove, and the bond length (L_b).

In general, all the analyzed parameters (maximum pullout force, ratio between maximum pullout force and FRP strength, loaded and free ends slips, average bond stress strengths) are very consistent yielding to low values of the corresponding coefficients of variation (CoV). However, high values of CoV were obtained for the case of slip at the loaded and free ends.

The pullout force, the loaded and free ends slips and the ratio between maximum pullout force and the FRP strength have increased with L_b, while the bond strength has decreased with the increase of L_b. A rougher surface has provided a better bond performance, as well as a deeper installation of the GFRP rod into the groove.

Failure modes included glulam shear failure, glulam/adhesive interfacial sliding, and FRP/adhesive interfacial sliding plus adhesive splitting.

Acknowledgements

This work is supported by FEDER funds through the Operational Programme for Competitiveness Factors - COMPETE and National Funds through FCT – Portuguese Foundation for Science and Technology under the project PTDC/ECM/74337/2006. The authors also like to thank all the companies that have been involved supporting and contributing for the development of this study, mainly: INEGI, S&P Clever Reinforcement, Portilame, MAPEI and Rothoblaas.

References

ACI 440.2R-08 (2008). “Guide for the Design and Construction of Externally Bonded FRP Systems for Strengthening Concrete Structures”, *Reported by ACI Committee 440*, American Concrete Institute, 80 pp.

Bank, L.C. (2004). “Mechanically-Fastened FRP (MF-FRP) – A Viable Alternative for Strengthening RC Members”, *Proceedings of CICE 2004*, Adelaide, Australia, 12 pp.

Barros, J.A.O.; Costa, I.G. (2010). “Bond Tests on Near Surface Reinforcement Strengthening for Concrete Structures”, *EN-CORE/fib Round Robin Testing Initiative*, Report 09.DEC/E-30 Department of Civil Engineering, University of Minho.

Costa, I.G.; Barros, J.A.O. (2001). “Assessment of the bond behavior of NSM FRP materials by pullout tests”, *First Middle East Conference on Smart Monitoring, Assessment and Rehabilitation of Civil Structures*, Dubai, February.

EN 408 (2003). “Timber structures - Structural timber and glued laminated timber. Determination of some physical and mechanical properties.” *European Committee for Standardization* (CEN), 31 pp.

ISO 527-2 (1993). “Plastics - Determination of tensile properties - Part 2: Test conditions for molding and extrusion plastics.” *International Organization for Standardization* (CEN).

ISO TC 71/SC 6 N Part 1 (2003). “Non-conventional reinforcement of concrete-test methods: Fiber reinforced polymer (FRP) bars.” *International Organization for Standardization* (CEN), 48 pp.